

# Gapped optical excitations from gapless phases: imperfect nesting in unconventional density waves

Balázs Dóra\* and András Ványolos

*Department of Physics, Budapest University of Technology and Economics, H-1521 Budapest, Hungary*

Kazumi Maki

*Department of Physics and Astronomy, University of Southern California, Los Angeles CA 90089-0484, USA*

Attila Virosztek

*Department of Physics, Budapest University of Technology and Economics, H-1521 Budapest, Hungary and  
Research Institute for Solid State Physics and Optics, P.O.Box 49, H-1525 Budapest, Hungary*

(Dated: November 12, 2018)

We consider the effect of imperfect nesting in quasi-one-dimensional unconventional density waves in the case, when the imperfect nesting and the gap depends on the same wavevector component. The phase diagram is very similar to that in a conventional density wave. The density of states is highly asymmetric with respect to the Fermi energy. The optical conductivity at  $T = 0$  remains unchanged for small deviations from perfect nesting. For higher imperfect nesting parameter, an optical gap opens, and considerable amount of spectral weight is transferred to higher frequencies. This makes the optical response of our system very similar to that of a conventional density wave. Qualitatively similar results are expected in d-density waves.

PACS numbers: 75.30.Fv, 71.45.Lr, 72.15.Eb, 72.15.Nj

## I. INTRODUCTION

The basic ingredient of the density wave (DW) formation is a band structure consisting of a pair of Fermi sheets, which can be nested to each other with a certain wavevector, giving rise to the density wave instability<sup>1</sup>. In real materials, however, this condition is not perfectly fulfilled:  $\varepsilon(\mathbf{k}) + \varepsilon(\mathbf{k} - \mathbf{Q}) \neq 0$ . In quasi-one-dimensional models studied during the early history of DW, one can choose it as  $\varepsilon(\mathbf{k}) + \varepsilon(\mathbf{k} - \mathbf{Q}) = 2\epsilon_0 \cos(2bk_y)$ , which shows the deviation from the one dimensionality<sup>2,3</sup>. In conventional CDW such as NbSe<sub>3</sub>, the depression of the transition temperature under pressure is described in terms of the pressure dependence of imperfect nesting, and the large ratio of  $2\Delta/T_c$  is also interpreted<sup>4,5,6</sup>. Similarly in field-induced SDW many features are successfully described by this model<sup>3</sup>. The general consequence of  $\epsilon_0$  is the destruction of the density wave phase: imperfect nesting depresses the DW transition temperature and destroys completely the density wave when  $\epsilon_0$  becomes larger than a critical value. Also the imperfect nesting term gives rise to dip structures in the angular dependent magnetoresistance in  $\alpha$ -(BEDT-TTF)<sub>2</sub>KHg(SCN)<sub>4</sub><sup>7</sup> and Bechgaard salts (TMTSF)<sub>2</sub>PF<sub>6</sub><sup>8</sup>. This motivates us to incorporate the effect of imperfect nesting in unconventional density wave (UDW) theory. UDW is a density wave, whose gap function depends on the wavevector, vanishes on certain points of the Fermi surface, allowing for low energy excitations. The average of the gap over the Fermi surface is zero, causing the lack of periodic modulation of the charge and spin density. Such systems have been studied and proposed over the years in a variety of systems<sup>9,10</sup>. These include heavy fermions like URu<sub>2</sub>Si<sub>2</sub><sup>11,12,13</sup>, CeCoIn<sub>5</sub><sup>14</sup>, organic conductors as  $\alpha$ -(BEDT-TTF)<sub>2</sub>KHg(SCN)<sub>4</sub><sup>15</sup> and (TMTSF)<sub>2</sub>PF<sub>6</sub><sup>8</sup>, high  $T_c$  superconductors<sup>16,17,18</sup>. Two different models are possible: 2D or 3D when the gap and the imperfect nesting depends on the same or different wavevector component, respectively. Previously we have analyzed the properties of the 3D model<sup>19</sup>, and now we turn to the investigation of the 2D one.

The object of the present paper is to extend the analysis of Refs. 19,20 to the presence of imperfect nesting when the gap and the imperfect nesting depends on the same wavevector component. We discuss the temperature dependence of the order parameter for different  $\epsilon_0$ 's. The phase boundary is almost the same as in a conventional DW. The chemical potential is shifted from its original value of the metallic state due to the presence of imperfect nesting. The temperature dependence of the order parameter,  $\Delta(T, \epsilon_0)$  is anomalous: although it decreases monotonically with increasing temperature, but exhibits a sharp cusp at  $\Delta(T, \epsilon_0) = 2\epsilon_0$ . In the density of states (DOS) the particle-hole symmetry is broken for the 2D model, leading to asymmetric density of states with respect to the Fermi energy. For high values of  $\epsilon_0$ , the zero of the density of states at the Fermi energy disappears, and DOS becomes finite for all energies. The optical conductivity is not affected by the deterioration of perfect nesting in a wide parameter range. By further increasing  $\epsilon_0$ , the divergent peak at  $2\Delta$  is divided into two new peaks. Moreover, a finite optical gap shows up at  $T = 0$  in spite of the finite density of states. Similar behaviour was identified in two dimensional UDW (the so-called d-density wave<sup>16</sup>): deviations from perfect nesting induce a finite optical gap<sup>21</sup>. In clean systems, the weight

of the Dirac delta peak at zero frequency is finite for all temperatures. We expect similar results in d-density waves as well.

## II. PHASE DIAGRAM

The single-particle electron thermal Green's function of UDW is given by<sup>22,23</sup>

$$G^{-1}(\mathbf{k}, i\omega_n) = i\omega_n - \xi(\mathbf{k})\rho_3 - \rho_1\sigma_3\text{Re}\Delta(\mathbf{k}) - \rho_2\sigma_3\text{Im}\Delta(\mathbf{k}), \quad (1)$$

where  $\rho_i$  and  $\sigma_i$  ( $i = 1, 2, 3$ ) are the Pauli matrices acting on momentum and spin space, respectively, and for UCDW  $\sigma_3$  should be replaced by 1.  $\Delta(\mathbf{k}) = \Delta e^{i\phi} \cos(bk_y)$  or  $\sin(bk_y)$ .  $\phi$  is the unrestricted phase (due to incommensurability) of the density wave, but its explicit value turns out to be irrelevant for our discussion,  $\xi(\mathbf{k})$  is the kinetic energy spectrum,  $\omega_n$  is the fermionic Matsubara frequency. The effect of imperfect nesting is incorporated in the theory by replacing the Matsubara frequency in the single particle Green's function with  $\omega_n + i(\epsilon_0 \cos(2bk_y) - \delta\mu)^{24,25}$ , where  $\delta\mu$  is the change of the chemical potential due to the change in the spectrum. The order parameter<sup>22</sup> is assumed to depend on the wavevector like  $\Delta(\mathbf{k}) = \Delta \sin(bk_y)$  or  $\Delta \cos(bk_y)$ . The second order phase boundary is given by  $\epsilon_0 = \Delta_0(T_c)$ , where  $\Delta_0(T)$  is the temperature dependence of the gap in a perfectly nested conventional DW with  $T_{c0}$  transition temperature.  $T_{c0}$  is the transition temperature in the absence of imperfect nesting. This is almost the complete phase diagram. At high temperature when  $T$  becomes of order of  $\epsilon_0$  the deviation from perfect nesting becomes irrelevant and the best nesting vector is  $\mathbf{Q} = (2k_F, \pi/b, \pi/c)$ . In the conventional scenario two DW phases can occur<sup>26</sup>, characterized by slightly different wave vectors and  $\mathbf{Q}$  is replaced by a temperature dependent wave vector, opening a narrow region above the critical nesting at low temperatures. For the present model, the possibility of ordering with different wave vector is there, although its examination is beyond the scope of the present discussion. The critical nesting is given by  $\epsilon_0 = \sqrt{e}\Delta_{00}/2 \approx 0.82\Delta_{00}$ , where  $\Delta_{00}$  is the gap in a perfectly nested system at zero temperature. The order parameter remains unchanged for  $\epsilon_0 < \Delta_{00}/2$ , and vanishes sharply as  $\epsilon_0$  approaches its critical value. This together with the phase diagram is shown in Fig. 1. The most interesting consequence of

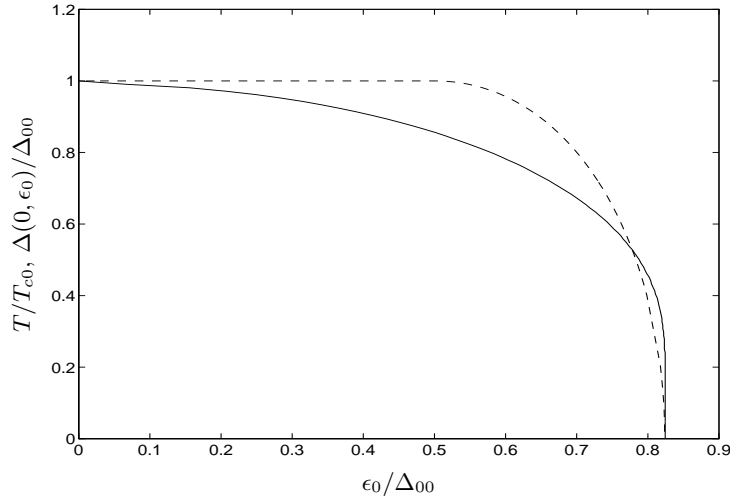


FIG. 1: The phase diagram (solid line) and the zero temperature order parameter (dashed line) are plotted in the presence of imperfect nesting.

imperfect nesting is that the chemical potential does not remain constant under the density wave formation. Its shift is given by  $\delta\mu = \epsilon_0\Theta(\Delta(T, \epsilon_0) - 2\epsilon_0) + \Delta(T, \epsilon_0)^2/(4\epsilon_0)\Theta(2\epsilon_0 - \Delta(T, \epsilon_0))$ , where  $\Theta(x)$  is the heaviside function. This behaviour can readily be seen from the density of states, where for any finite  $\Delta$  the total number of states below the Fermi energy is regained only by shifting the Fermi energy as given above. Note that this change belongs to a sinusoidal gap while for a cosinusoidal gap the sign of the shift is reversed. The change in the spectrum in the presence of imperfect nesting is shown in Fig. 2, which is given by

$$E_{\pm}(\mathbf{k}) = \frac{\varepsilon(\mathbf{k}) + \varepsilon(\mathbf{k} - \mathbf{Q})}{2} \pm \sqrt{\left(\frac{\varepsilon(\mathbf{k}) - \varepsilon(\mathbf{k} - \mathbf{Q})}{2}\right)^2 + |\Delta(\mathbf{k})|^2}. \quad (2)$$

In the perfectly nested case, the low energy part of the spectrum consists of Dirac cones with peaks at the Fermi energy<sup>20</sup>. For small  $\epsilon_0$ , the spectrum is still crossed by the Fermi energy at the zeros of the gap. By increasing  $\epsilon_0$ , a broad bump develops in the upper band, and crosses the Fermi energy. At this point, a large number of possible states becomes available, and the chemical potential starts decreasing to keep the total number of particles unchanged.

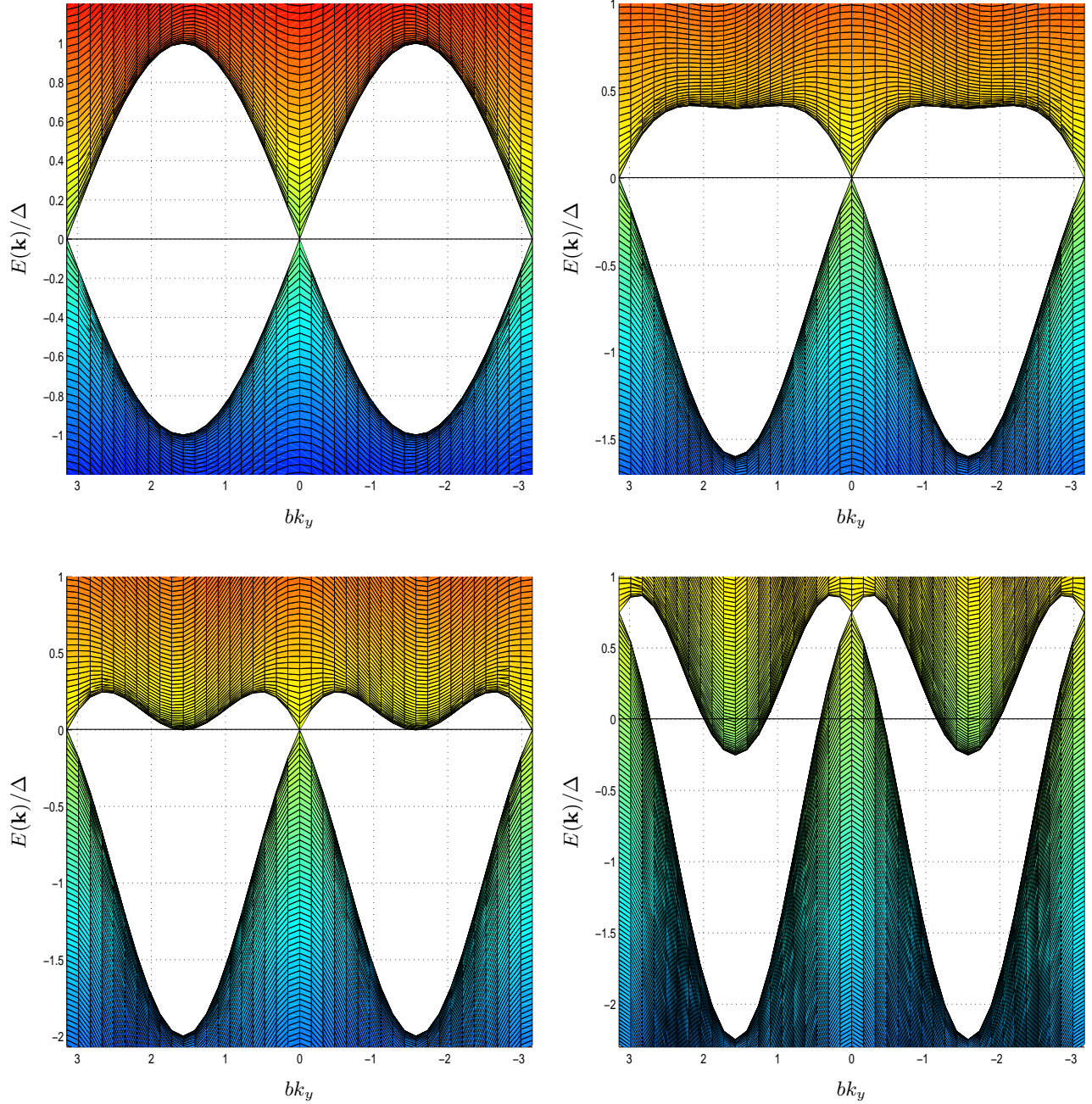


FIG. 2: The evolution of the quasiparticle spectrum is shown, viewed from the direction of the  $k_x$  axis, for  $\Delta(\mathbf{k}) = \Delta \sin(bk_y)$  in the presence of imperfect nesting for  $\epsilon_0/\Delta = 0, 0.3, 0.5$  and  $1$  from left to right, top to bottom. The horizontal line denotes the Fermi energy. The band structure is chosen as  $\varepsilon(\mathbf{k}) = -2t_a \cos(ak_x) - 2t_b \cos(bk_y) + \epsilon_0 \cos(2bk_y)$  with parameters as  $t_a/\Delta = 2$ ,  $t_b/\Delta = 0.1$  at half filling.

A direct consequence of this shift is a cusp in the temperature dependence of  $\Delta$  at  $\Delta = 2\epsilon_0$ , since at this point the chemical potential changes. This feature is shown in Fig. 3, which is obtained from the numerical solution of the gap

equation:

$$1 = TV \frac{N_0}{4} \sum_n \int_0^{2\pi} \frac{\sin^2(y) dy}{\sqrt{(\omega_n + i(\epsilon_0 \cos(2y) - \delta\mu))^2 + \Delta^2 \sin^2(y)}}, \quad (3)$$

where  $V > 0$  is the interaction responsible for the UDW formation,  $N_0$  is the density of states in the normal state at the Fermi energy per spin.

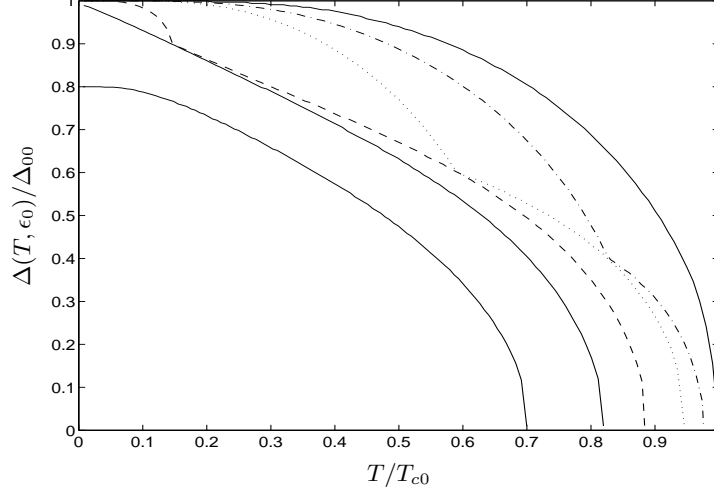


FIG. 3: The temperature dependence of the order parameter for the 2D model is shown for  $\epsilon_0/\Delta_{00} = 0, 0.2, 0.3, 0.45, 0.55$  and  $0.7$  from right to left. The cusp shows up only for  $2\epsilon_0 < \Delta_{00}$ .

### III. DENSITY OF STATES

The quasi-particle density of states is given by

$$g_{2D}(E) = N(x, a) = N_0 \int_0^{2\pi} \frac{dy}{2\pi} \text{Re} \frac{|E + \delta\mu - \epsilon_0 \cos(2y)|}{\sqrt{(E + \delta\mu - \epsilon_0 \cos(2y))^2 - \Delta^2 \sin^2(y)}}. \quad (4)$$

The energy variables are expressed in units of  $\epsilon_0$ , i.e.  $a = \Delta/\epsilon_0$  and  $x = (E + \delta\mu)/\epsilon_0$ , the energy is measured from the new Fermi energy. The density of states is obtained as

$$N(x, a) = N_0 \frac{1}{\pi \sqrt{pq}} \left( \left( x - 1 - \frac{2q}{p - q} \right) K \left( \frac{1}{2} \sqrt{\frac{1 - (p - q)^2}{pq}} \right) + \frac{p + q}{p - q} \Pi \left( \frac{(p - q)^2}{-4pq}, \frac{1}{2} \sqrt{\frac{1 - (p - q)^2}{pq}} \right) \right) \quad (5)$$

for  $x > a^2/8 + 1$ , where  $p = \sqrt{(m - 1)^2 + n^2}$ ,  $q = \sqrt{m^2 + n^2}$ ,  $m = (a^2 - 4(x - 1))/8$ ,  $n = a\sqrt{-a^2 + 8(x - 1)}/8$ ,  $K(z)$  and  $\Pi(n, z)$  are the complete elliptic integrals of the first and third kind<sup>27</sup>. In the remaining regions the DOS reads as

$$\begin{aligned} N(x, a) &= N_0 (\Theta(a - 4)f_1(x, a) + \Theta(4 - a)f_3(x, a)), \quad \frac{a^2}{8} + 1 > x > a - 1, \\ N(x, a) &= N_0 \text{sgn}(x - 1)f_2(x, a), \quad a - 1 > x > -a - 1, \\ N(x, a) &= -N_0 f_3(x, a), \quad -a - 1 > x, \end{aligned} \quad (6)$$

where the following notations are used:

$$f_1(x, a) = \frac{1}{\pi \sqrt{(y_2 - 1)y_1}} \left( (x - 1 + 2y_2)K \left( \sqrt{\frac{y_2 - y_1}{(y_2 - 1)y_1}} \right) - 2y_2 \Pi \left( \frac{1}{1 - y_2}, \sqrt{\frac{y_2 - y_1}{(y_2 - 1)y_1}} \right) \right), \quad (7)$$

$$f_2(x, a) = \frac{1}{\pi\sqrt{y_2 - y_1}} \left( (x - 1 + 2y_2)K \left( \sqrt{\frac{(y_2 - 1)y_1}{y_2 - y_1}} \right) - 2y_2\Pi \left( \frac{y_1}{y_1 - y_2}, \sqrt{\frac{(y_2 - 1)y_1}{y_2 - y_1}} \right) \right), \quad (8)$$

$$f_3(x, a) = \frac{1}{\pi\sqrt{(1 - y_1)y_2}} \left( 2(y_2 - y_1)\Pi \left( \frac{y_2 - 1}{y_1 - 1}, \sqrt{\frac{(1 - y_2)y_1}{(1 - y_1)y_2}} \right) - 2\text{sgn}(x - 1)\Pi \left( \frac{y_1}{y_1 - 1}, \sqrt{\frac{(1 - y_2)y_1}{(1 - y_1)y_2}} \right) + \right. \\ \left. + (x - 1 + 2y_1 + \text{sgn}(x - 1)(x + 1))K \left( \sqrt{\frac{(1 - y_2)y_1}{(1 - y_1)y_2}} \right) \right), \quad (9)$$

and  $y_1 = (a^2 - 4(x - 1) - a\sqrt{a^2 - 8(x - 1)})/8$ ,  $y_2 = (a^2 - 4(x - 1) + a\sqrt{a^2 - 8(x - 1)})/8$ .

The particle-hole symmetry is broken, which can be readily seen from the behaviour of the peaks in the density of states, which slide from  $\pm\Delta$  to  $-\Delta - \epsilon_0 - \delta\mu$  below the Fermi surface, while above it to  $\Delta - \epsilon_0 - \delta\mu$  for  $4\epsilon_0 < \Delta$  and to  $\epsilon_0 + \Delta^2/8\epsilon_0 - \delta\mu$  otherwise. Also the zero in DOS is at the new Fermi energy for  $\epsilon_0 < \Delta/2$ , and for larger  $\epsilon_0$  there exists no zero in the DOS. The density of states is plotted in Fig. 4. These statements correspond to  $\Delta(\mathbf{k}) = \Delta \sin(k_y b)$ , while for a cosinusoidal gap  $E \rightarrow -E$  change is needed in the density of states.

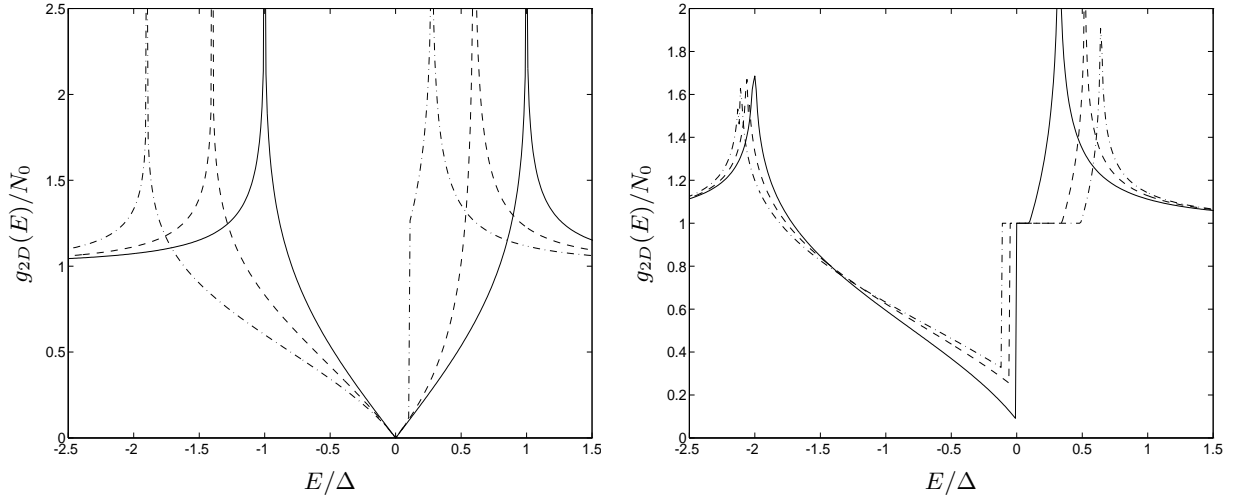


FIG. 4: The density of states as a function of energy is shown in the left panel for  $\epsilon_0/\Delta = 0$  (solid line), 0.2 (dashed line), 0.45 (dashed-dotted line). In the right panel  $\epsilon_0/\Delta = 0.55$  (solid line), 0.7 (dashed line) and 0.8 (dashed-dotted line) are used.

The residual density of states (i.e.  $g_{2D}(E = 0)$ ) is given by  $N_0\Theta(2\epsilon_0 - \Delta)$ . Since on the Fermi surface the DOS vanishes in the same way for  $\epsilon_0 \ll \Delta_0$  than in the perfectly nested case, the specific heat increases quadratically with temperature close to  $T = 0$  K in this region, while for large  $\epsilon_0$  it equals to the specific heat in the normal state.

#### IV. OPTICAL CONDUCTIVITY

In this section we investigate the quasiparticle contribution to the optical conductivity. For simplicity we neglect the effect of the quasiparticle damping due to impurity scattering for example. The quasiparticle part of the conductivity contains relevant information about the system in the perpendicular cases ( $y$  and  $z$ ) when the effect of the collective contributions can be neglected. The regular part of the optical conductivity (without the Dirac delta) is given by

$$\text{Re}\sigma_{\alpha\beta}^{\text{reg}}(\omega) = N_0 \frac{\pi e^2}{\omega^2} \int_{-\pi}^{\pi} \frac{d(bk_y)}{2\pi} \int_{-\pi}^{\pi} \frac{d(ck_z)}{2\pi} \text{Re} \frac{v_\alpha(\mathbf{k})v_\beta(\mathbf{k})\Delta^2(\mathbf{k})}{\sqrt{(\omega/2)^2 - \Delta^2(\mathbf{k})}} \left( \tanh\left(\frac{|\omega| - 2\eta}{4T}\right) + \tanh\left(\frac{|\omega| + 2\eta}{4T}\right) \right), \quad (10)$$

where  $v_\alpha(\mathbf{k})$  is the quasiparticle velocity in the  $\alpha$  direction,  $v_x = v_F$ ,  $v_y = \sqrt{2}t_b b$ ,  $v_z = \sqrt{2}t_c c$  and  $\eta = \epsilon_0 \cos(2bk_y) - \delta\mu$ . From now on we restrict our investigation to the  $T = 0$  K case. The optical conductivity remains the same as in

the perfectly nested case for  $2\epsilon_0 < \Delta(0, \epsilon_0) = \Delta_{00}$ . For higher  $\epsilon_0$  the optical conductivity is zero for  $\omega < G$ ,  $G = \Delta(\sqrt{8-a^2}-a)/2$  similarly to the effect of magnetic field where the  $\omega < 2\mu_B H$  part of the conductivity is chopped<sup>28</sup>, in other words a clean optical gap develops. This can readily be observed in Fig. 2: when the upper band crosses the Fermi energy, the chemical potential moves below the zeros of the gap, suppressing the low energy excitations, since only  $\mathbf{q} = \mathbf{0}$  transitions are allowed for. Parallel to this the peak at  $2\Delta$  splits into 2 new peaks at  $\Delta(\sqrt{8-a^2}+a)/2$  and at  $\Delta(a/2+2/a)$ . For  $\omega > 2\epsilon_0(1+a^2/4)$  the optical conductivity remains unchanged compared to Ref. 20. The only change in the remaining region can be expressed by redefining the  $I$  functions<sup>20</sup>:

$$I(\alpha, \beta, g) = \frac{\omega^2 g}{4\Delta^2} \left( F(g\sqrt{\beta}, x) - F(g\sqrt{\alpha}, x) - E(g\sqrt{\beta}, x) + E(g\sqrt{\alpha}, x) \right) \quad (11)$$

$$I_{sin}(\alpha, \beta, g) = \frac{\omega}{12\Delta} \left( \sqrt{\beta(1-\beta)} \left( \left( \frac{\omega}{\Delta} \right)^2 - 4\beta^2 \right) - \sqrt{\alpha(1-\alpha)} \left( \left( \frac{\omega}{\Delta} \right)^2 - 4\alpha^2 \right) + \left( \frac{\omega}{\Delta g} + \frac{1}{2} \left( \frac{\omega g}{\Delta} \right)^3 \right) \left( F(g\sqrt{\beta}, x) - F(g\sqrt{\alpha}, x) \right) - \left( \frac{2\omega g}{\Delta} + \frac{g}{2} \left( \frac{\omega}{\Delta} \right)^3 \right) \left( E(g\sqrt{\beta}, x) + E(g\sqrt{\alpha}, x) \right) \right) \quad (12)$$

and  $I_{cos}(\alpha, \beta, g) = I(\alpha, \beta, g) - I_{sin}(\alpha, \beta, g)$ , where  $F(z, k)$  and  $E(z, k)$  are the incomplete elliptic integrals of the first and second kind,  $x = 2\Delta/\omega g^2$  and the arguments of the  $I$  functions are obtained as

$$\alpha = \max \left( 0, \frac{1}{2} - \frac{a^2}{8} - \frac{a\omega}{4\Delta} \right) \quad (13)$$

$$\beta = \min \left( 1, \frac{1}{2} - \frac{a^2}{8} + \frac{a\omega}{4\Delta}, \left( \frac{\omega}{2\Delta} \right)^2 \right) \quad (14)$$

$$g = \max \left( 1, \frac{2\Delta}{\omega} \right) \quad (15)$$

for  $\omega > G$  and for  $a < 2$ . For  $a > 2$ ,  $\alpha = 0$ ,  $\beta = 1$  and the  $I$  functions reduce to those in Ref. 20. Here min and max gives the largest and the smallest value of its arguments, respectively. With these notations the optical conductivity reads as

$$\text{Re}\sigma_{yy}^{sin,cos}(\omega) = e^2 N_0 v_y^2 \frac{8\Delta(0, \epsilon_0)^2}{\omega^3} I_{sin,cos}(\alpha, \beta, g), \quad (16)$$

$$\text{Re}\sigma_{zz}(\omega) = e^2 N_0 v_z^2 \frac{4\Delta(0, \epsilon_0)^2}{\omega^3} I(\alpha, \beta, g). \quad (17)$$

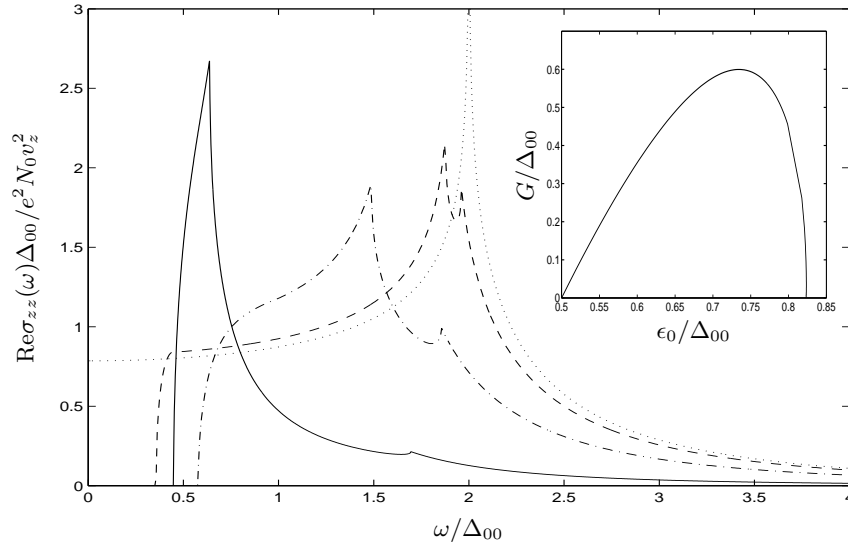


FIG. 5: The real part of the complex conductivity for the 2D model in the  $z$  direction is shown for  $\epsilon_0/\Delta_{00} = 0 - 0.5$  (dotted line), 0.6 (dashed line), 0.7 (dashed-dotted line) and 0.8 (solid line). Note that the same curves belong to  $\sigma_{xx}(\omega)$  by changing  $v_z$  to  $v_F$ . The inset shows the  $\epsilon_0$  dependence of the optical gap.

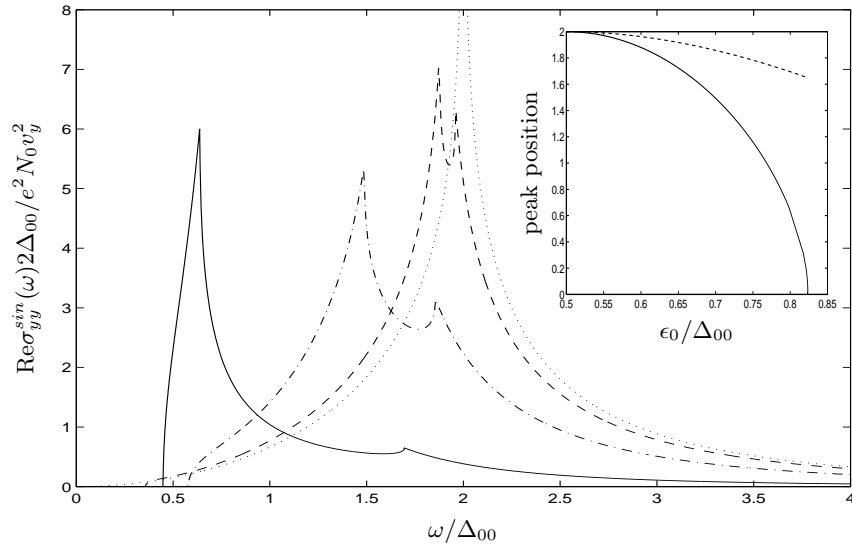


FIG. 6: The real part of the complex conductivity for the 2D model for a sinusoidal gap in the  $y$  direction is shown for  $\epsilon_0/\Delta_{00} = 0 - 0.5$  (dotted line), 0.6 (dashed line), 0.7 (dashed-dotted line) and 0.8 (solid line). The inset shows the  $\epsilon_0$  dependence of the peaks.

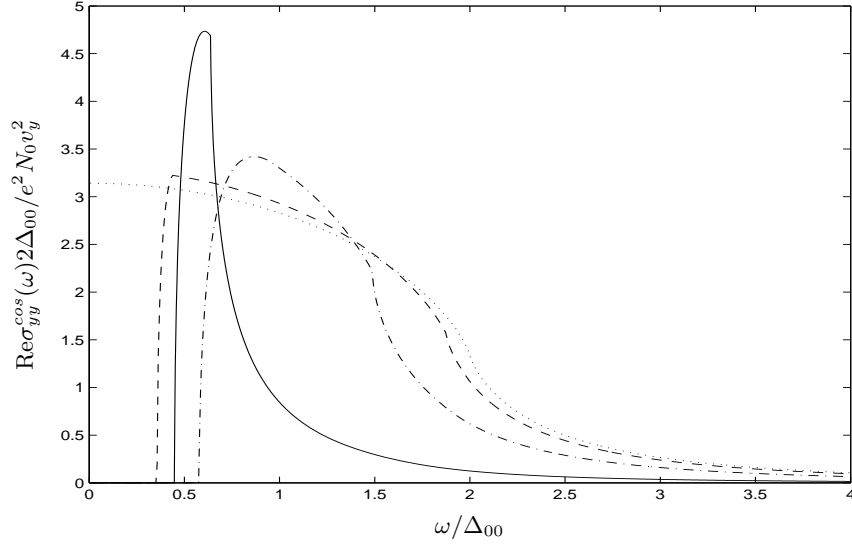


FIG. 7: The real part of the complex conductivity for the 2D model for a cosinusoidal gap in the  $y$  direction is shown for  $\epsilon_0/\Delta_{00} = 0$  (dotted line), 0.6 (dashed line), 0.7 (dashed-dotted line) and 0.8 (solid line).

The optical conductivity in the three qualitatively different cases is shown in Figs. 5, 6, 7. In the  $x$  direction the quasiparticle part of the optical conductivity is the same as  $\sigma_{zz}(\omega)$  if we replace  $v_z$  with  $v_F$ , although in the  $x$  direction it does not give the total conductivity since collective contributions change significantly the quasiparticle part as it was shown in Ref. 29. At first sight the sum rule seems to be violated since a lot of optical weight is missing at small frequencies below the optical gap. But the  $\delta(\omega)$  part of the conductivity does not freeze out at  $T \rightarrow 0$  in the presence of imperfect nesting, and its coefficient provides the missing area. As is well known, in the presence of impurity scattering,  $\delta(\omega)$  changes to a Drude like peak centered at  $\omega = 0$ . At finite temperature, the optical gap vanishes, but excitations below  $G$  are only possible with a probability of  $\sim \exp(-(\epsilon_0 - \Delta^2/(4\epsilon_0))/T)$ .

## V. CONCLUSION

We have studied theoretically the effect of imperfect nesting in unconventional density waves. Two qualitatively different cases are possible: the gap and imperfect nesting depend on the same (called 2D model) or different wave

vector component (3D case)<sup>19</sup>. Here we concentrated on the former. We explored the phase diagram which is identical to the one in conventional density wave. The zero temperature gap coefficient is not constant contrary to the conventional case. The chemical potential changes compared to the normal state value. The density of states turned out to be asymmetric with respect to the Fermi energy due to the particle-hole symmetry breaking, but the logarithmically divergent peaks of the  $\epsilon_0 = 0$  case remain present, but at different energies. For larger values of imperfect nesting ( $2\epsilon_0 > \Delta(T, \epsilon_0)$ ), the zero at the Fermi energy disappears, and the low energy density of states regains its normal state form. Usually  $\epsilon_0$  is thought to vary with pressure providing the opportunity to check these result in a wide range of parameters. The optical gap of the model in the perpendicular optical conductivity can be observed experimentally at low temperatures. Moreover the splitting and lowering of the resonant peak at  $\omega = 2\Delta$  (when the wavevector dependence of the gap and the velocity coincide) or its absence (for the other kind of gap)<sup>19</sup> could provide robust signatures of the microscopic nature of the low temperature phase.

### Acknowledgments

This work was supported by the Magyary Zoltán postdoctoral program of Foundation for Hungarian Higher Education and Research (AMFK) and by the Hungarian Scientific Research Fund under grant numbers OTKA TS040878, T046269 and NDF45172.

---

\* Electronic address: dora@kapica.phy.bme.hu

- <sup>1</sup> G. Grüner, *Density waves in solids* (Addison-Wesley, Reading, 1994).
- <sup>2</sup> G. Mihály, A. Virosztek, and G. Grüner, Phys. Rev. B **55**, R13456 (1997).
- <sup>3</sup> T. Ishiguro, K. Yamaji, and G. Saito, *Organic Superconductors* (Springer, Berlin, 1998).
- <sup>4</sup> K. Yamaji, J. Phys. Soc. Jpn. **51**, 2787 (1982).
- <sup>5</sup> K. Yamaji, J. Phys. Soc. Jpn. **52**, 1361 (1983).
- <sup>6</sup> X. Huang and K. Maki, Phys. Rev. B **40**, 2575 (1989).
- <sup>7</sup> K. Maki, B. Dóra, M. V. Kartsovnik, A. Virosztek, B. Korin-Hamzić, and M. Basletić, Phys. Rev. Lett. **90**, 256402 (2003).
- <sup>8</sup> B. Dóra, K. Maki, A. Ványolos, and A. Virosztek, Europhys. Lett. **67**, 1024 (2004).
- <sup>9</sup> A. H. Castro-Neto, Phys. Rev. Lett. **86**, 4382 (2001).
- <sup>10</sup> A. A. Nersisyan and G. E. Vachnadze, J. Low T. Phys. **77**, 293 (1989).
- <sup>11</sup> H. Ikeda and Y. Ohashi, Phys. Rev. Lett. **81**, 3723 (1998).
- <sup>12</sup> A. Virosztek, K. Maki, and B. Dóra, Int. J. Mod. Phys. B **16**, 1667 (2002).
- <sup>13</sup> Zs. Gulácsi and M. Gulácsi, Phys. Rev. B **36**, 699 (1987).
- <sup>14</sup> B. Dóra, K. Maki, A. Virosztek, and A. Ványolos, cond-mat/0408351.
- <sup>15</sup> B. Dóra, K. Maki, and A. Virosztek, Mod. Phys. Lett. B **18**, 327 (2004).
- <sup>16</sup> S. Chakravarty, R. B. Laughlin, D. K. Morr, and C. Nayak, Phys. Rev. B **63**, 094503 (2001).
- <sup>17</sup> L. Benfatto, S. Caprara, and C. Di Castro, Eur. Phys. J. B **17**, 95 (2000).
- <sup>18</sup> K. Maki, B. Dóra, A. Virosztek, and A. Ványolos, Curr. Appl. Phys. **4**, 603 (2004).
- <sup>19</sup> B. Dóra, K. Maki, and A. Virosztek, Phys. Rev. B **66**, 165116 (2002).
- <sup>20</sup> B. Dóra and A. Virosztek, Eur. Phys. J. B **22**, 167 (2001).
- <sup>21</sup> D. N. Aristov and R. Zeyher, cond-mat/0406419.
- <sup>22</sup> B. Dóra, A. Virosztek, and K. Maki, Phys. Rev. B **66**, 115112 (2002).
- <sup>23</sup> K. Maki, Phys. Rev. B **33**, 4826 (1986).
- <sup>24</sup> X. Huang and K. Maki, Phys. Rev. B **42**, 6498 (1990).
- <sup>25</sup> X. Huang and K. Maki, Phys. Rev. B **46**, 162 (1992).
- <sup>26</sup> Y. Hasegawa and H. Fukuyama, J. Phys. Soc. Japan **55**, 3978 (1986).
- <sup>27</sup> P. F. Byrd and M. D. Friedman, *Handbook of elliptic integrals for engineers and physicist* (Springer-Verlag, Berlin, Göttingen, Heidelberg, 1954).
- <sup>28</sup> B. Dóra, A. Virosztek, and K. Maki, Phys. Rev. B **65**, 155119 (2002).
- <sup>29</sup> B. Dóra and A. Virosztek, Europhys. Lett **61**, 396 (2003).